ON THE MODELLING OF SINGLE-PHASE TURBULENT ENERGY TRANSPORT IN SUBCHANNELS

O. S. Eiff and M.F. Lightstone[1]
Department of Mechanical and Industrial Engineering
University of Toronto
5 King's College Road
Toronto, Ontario M5S 3G8

1. INTRODUCTION

Mathematical modelling of the heat transfer and fluid flow in nuclear fuel channels is integral to ensuring the safe operation and design of nuclear reactors. Since analytical solutions to the governing equations are not generally available, computational methods are used to provide numerical solutions to the equations. Further, because of the complex geometry of the fuel bundles and the appendages, detailed grid-independent numerical solutions of the fluid flow and heat transfer within each fuel bundle are not feasible on a routine basis.

An alternative to solving for the detailed description of the fluid flow and heat transfer is to average over larger control volumes and use constitutive relations to supply the information that was lost in the averaging process. This is the basis of subchannel codes. Figure 1 shows the subchannels for a 37-element CANDU fuel bundle. A subchannel is defined as the flow region bounded by the fuel rods and imaginary lines joining the fuel rod centroids. Control volumes are created by dividing each subchannel axially along the length of the bundle.

ASSERT-PV [1] (Advanced Solution of Subchannel Equations in Reactor Thermalhydraulics, Pressure-Velocity) is a subchannel code that is used widely in the Canadian nuclear industry. It is a transient, quasi-two-fluid computer code developed to predict the heat transfer and fluid flow in CANDU fuel bundles. ASSERT-PV solves the conservation equations for mass, momentum, and energy for the single or multi-phase mixture, as well as separate energy equations for the vapour and liquid phases. The elliptic form of the governing equations is used to allow for prediction of low and recirculating flows. The code has been used for a range of applications including forming the basis for the development of coolant mixing models [2] for safety analysis production codes such as FACTAR [3], assessing the impact of a channel flow blockage [4], as well for a range of critical heat flux assessments [5] [6].

As discussed above, since subchannel codes employ relatively large control volumes, the fine-grained details of the fluid flow and heat transfer are not resolved and constitutive relationships are required. In the solution of the momentum equations, for example, constitutive relationships are used to model the frictional losses due to the presence of walls, while bundle appendages such as endplates, spacers, and bearing pads are modelled by applying local k-factors. Solution of the thermal energy equation requires expressions for the heat transfer from the wall and between phases as well as an expression for the thermal mixing due to fluid turbulence.

The mathematical modelling of the turbulent transport of energy is the focus of this paper. The motivation for the work is to determine the validity of the available correlations for the case where steam is the working fluid. This is assessed through a survey of the literature for experimental data and mathematical models pertaining to turbulent thermal mixing, and by comparing predictions from the correlations to data obtained from water and air experiments.

[1]Please address all correspondence to M.F. Lightstone.

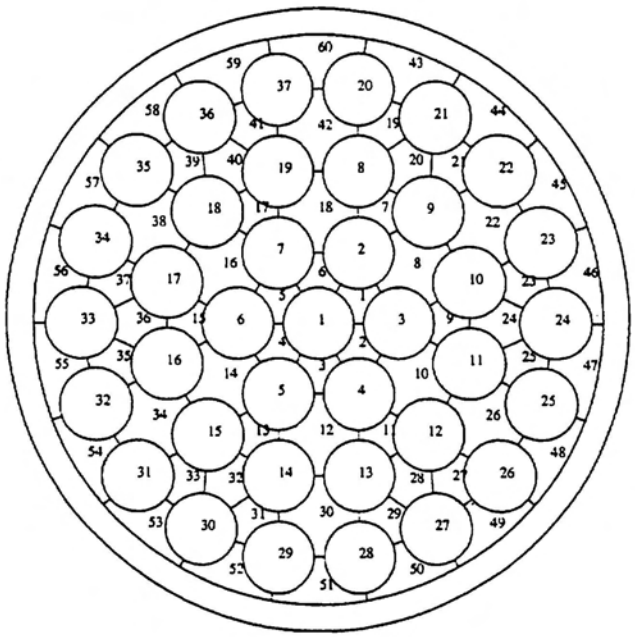

Figure 1: Subchannel Layout for a CANDU 37-Element Fuel Bundle

2. MODELLING OF TURBULENT TRANSPORT OF ENERGY

In a turbulent flow, the fluid velocities and enthalpies (for non-isothermal flows) become irregular and unpredictable. Such flows are usually modelled by decomposing the quantity of interest into a time-averaged plus a fluctuating component, *i.e.*, for the instantaneous velocity, v, and enthalpy, h:

$$v = \overline{v} + v' \quad \text{and} \quad h = \overline{h} + h' \tag{1}$$

where $\overline{v}$ and $\overline{h}$ are the time-averaged or mean values of the velocity and enthalpy, respectively, and v' and h' are the fluctuating components. By substituting these equations into the energy equation and time-averaging each term in the equation, an additional term representing turbulent transport will arise. This term, which involves a correlation between h' and v', must be modelled.

A standard approach used to model the transport due to turbulence is the gradient diffusion method:

$$q_t'' = \rho\overline{v'h'} = -\rho\varepsilon_t \frac{\partial \overline{h}}{\partial \psi}|_{i,j}, \tag{2}$$

where q_t'' is the heat transfer per unit area due to turbulent motion, ρ is the fluid density, ε_t is the turbulent diffusivity, and ψ represents the coordinate direction joining two adjacent subchannels i and j. The enthalpy gradient can be written as:

$$\frac{\partial \overline{h}}{\partial \psi}|_{i,j} = \frac{h_j - h_i}{z_{ij}} \tag{3}$$

where z_{ij} is the distance over which mixing occurs, and h_i and h_j are the time-averaged enthalpies in subchannels i and j respectively. Note that for convenience the overbar has been dropped. The total energy transport due to turbulent fluctuations is obtained by multiplying Equation (2) by the heat transfer area, A, between two adjacent subchannels. The heat transfer area is calculated

from $A = Lc$, where L is the length of a control volume and c is the width of the gap, yielding:

$$Q_{ij} = -A\rho\varepsilon_t \frac{h_j - h_i}{z_{ij}} = (Lc)\rho\frac{\varepsilon_t}{z_{ij}}(h_i - h_j). \tag{4}$$

The turbulent mixing rate, w'_{ij}, is introduced by rewriting Equation (4) as:

$$Q_{ij} = Lw'_{ij}(h_i - h_j) \tag{5}$$

where:

$$w'_{ij} = \rho c\frac{\varepsilon_t}{z_{ij}} \tag{6}$$

The quantity w'_{ij} is defined as an effective mass flow (per unit control volume length) due to the turbulence. Correlations are used to provide values for w'_{ij}.

3. CORRELATIONS FOR w'_{ij}

The turbulent mixing rate, w'_{ij}, depends on both the geometry of the subchannel pair and the Reynolds number of the flow. Hence, the convention is to write Equation (6) in the following form:

$$\frac{w'_{ij}}{\mu} = \frac{\rho c\varepsilon_t}{z_{ij}\mu} = \left(\frac{c}{d}\right)\left(\frac{d}{z_{ij}}\right)\left(\frac{\varepsilon_t}{\nu}\right) = \left(\frac{c}{d}\right)\cdot(\lambda_{ij})\cdot(f(Re)) \tag{7}$$

where:

d/z_{ij} $= \lambda_{ij}$ = a function of the subchannel geometry only
ε_t/ν = a function of Reynolds number only

In this paper a number of correlations for w'_{ij} are presented. These are the correlations of Rogers and co-workers [7] [8], Petrunik [9], and the more recent correlation of Rehme [10]. These correlations assume the same or very similar Reynolds number dependence, with the major difference in the correlations being in the λ_{ij} component of Equation (7). The general formulation for the Reynolds number dependence and correlations for λ_{ij} are presented in separate sections below.

3.1 Reynolds Number Formulation

The dependence of the mixing rate on the Reynolds number is found by considering classical flows such as those in open channels and smooth pipes. For fully developed turbulent open channel flows and for flows in the central portion of a circular tube, the turbulent diffusivity ν_t can be expressed as:

$$\nu_t \propto u^* D \tag{8}$$

where u^* is the friction velocity, and D is the hydraulic diameter of the channel or pipe. The Reynolds number dependence is introduced via the friction velocity, which is defined as:

$$u^* = \sqrt{\frac{\tau_w}{\rho}} \tag{9}$$

where τ_w is the wall shear stress:

$$\tau_w = \frac{1}{2}\rho f U^2 \tag{10}$$

and U and f are the average axial fluid velocity and the Fanning friction factor, respectively. For fully developed flow in smooth tubes, f is found from:

$$f = K_f Re^{-n} \tag{11}$$

where $K_f = 0.046$ and $n = 0.2$ [11]. Substituting Equations (9) to (11) into Equation (8) yields:

$$\nu_t \propto \nu Re^{1-n/2} \tag{12}$$

In order to relate the turbulent diffusion of momentum, ν_t, to the turbulent diffusion of energy, ε_t, the turbulent Prandtl number is presumed to be constant. Thus:

$$\frac{\varepsilon_t}{\nu} \propto Re^{1-n/2} \tag{13}$$

In the equation for w'_{ij}, the constants that would appear in the ε_t equation are absorbed into the correlations for λ_{ij}. This yields:

$$\frac{w'_{ij}}{\mu} = \left(\frac{c}{d}\right) \cdot (\lambda_{ij}) \cdot (Re^m) \tag{14}$$

where:

$$m = 1 - \frac{n}{2} \tag{15}$$

For $n = 0.2$, the exponent m in Equation (14) equals 0.9. Rogers and co-workers and Rehme use an exponent of 0.9 for the Reynolds number dependence in their correlations. Petrunik uses an exponent of 0.827.

Care must be taken in calculating a combined Reynolds number for the two adjacent subchannels for use in Equation (14). Differences in geometry or the presence of flow obstructions can result in different Reynolds numbers in the adjacent subchannels. There does not appear to be a uniform method used for calculating the combined Reynolds number since different researchers use alternative methods. Indeed, some researchers are ambiguous as to the method used to calculate that quantity. For adjacent subchannels of the same geometry, the Reynolds numbers in each subchannel should be the same. Differences in the Reynolds numbers will occur when the subchannels have different hydraulic diameters or are subjected to non-uniform obstructions. This problem is discussed further in Section 4.

3.2 Correlations for the Geometrical Parameter λ_{ij}

The geometrical parameters that impact on the mixing due to turbulence include the ratio of the gap spacing to rod diameter (c/d), the shape of the subchannel pair, and the presence of bundle appendages. Subchannel shapes in the bundle interior are classified as triangular or square (see, for example, subchannels 28 and 10 in Figure 1). As a result of the two subchannel types, three subchannel-pair configurations are identified. These are triangle-triangle (T-T), square-square (S-S), and square-triangle (S-T). Examples of T-T, S-S, and S-T configurations are given by subchannels pairs (9,24), (10,26), and (10,11) in Figure 1. The square subchannels adjacent to the pressure tube wall represent a third type of subchannel. For the purposes of calculating turbulent transport, these subchannels are normally treated as square.

Bundle appendages impact on thermal mixing via two mechanisms. Firstly, they create a mean diversion crossflow induced via radial pressure gradients. Energy is therefore advected between adjacent subchannels by the mean radial flow. Secondly, bundle appendages promote fluid turbulence by increasing the production of turbulent kinetic energy. Hence correlations derived

Table 1: Summary of Experimental Conditions

	Rogers (bundle)	Rogers (S-S)	Rogers (S-T)	Rogers (T-T)	Rehme	Petrunik
subchannel types	S-S, S-T T-T	S-S	S-T	T-T	S-S, S-T T-T	S-S, S-T T-T
no. of studies	8	3	3	3	24	5
no. of points	44	57	33	106	41	53
c/d	0.083 to 0.4	0.0355 to 1.108	.035 to 0.149	0.033 to 0.4	0.011 to 0.83	0.035 to ?
Reynolds No. ($\times 10^{-3}$)	2.5 to 127	14 to 150	26 to 130	1.35 to 70	1.35 to 70+	6.0 to ?
Fluids	air, H_2O Freon	air, H_2O	H_2O	air, H_2O	air, H_2O Freon, ...	air, H_2O Genetron-12

from experiments where appendages were present (i.e., 'bundle' correlations) should be distinguished from those obtained from clean or 'simple' geometries. The correlations of Rogers and co-workers [7] [8], Petrunik [9], and Rehme [10] are discussed in turn below. The experimental conditions used for each of the correlations is summarised in Table 1 and a summary of the formulations for λ_{ij} is presented in Table 2.

3.2.1 Correlation of Rogers and Co-Workers. In this section the correlations of Rogers and Rosehart [7] and Rogers and Tahir [8] are presented. Rogers and Rosehart distinguish between 'simple' and 'bundle' geometries whereas Petrunik and Rehme do not. It should be noted that in this study it was not possible to assess the conditions distinguishing the simple versus the bundle geometries, since most of the data on which Rogers and co-workers based their results are published in inaccessible reports during the 1960's. However, even in Rogers and Tahir's study of a simple T-T bundle, it is not clear how the rods are supported, except that the authors note the walls are supported by rigid yokes at a spacing of about 0.6 m (equal to 24 rod diameters). This implies that even in supposedly 'simple' experiments, there are 'bundle' type conditions to be found - as expected in any physical experiment.

Bundle Geometries

For bundle geometries, Rogers and Rosehart propose that

$$\lambda_{ij} = K \left(\frac{c}{d}\right)^{-r} \tag{16}$$

Values for the constants K and r in Equation (16) were found by considering eight different studies (for a total of 44 points). These studies included data of all subchannel types, with working fluids of air, water and Freon. From these experiments, values of $K = 0.0058$ and $r = 1.46$ were deduced. Their correlation is limited to c/d values of 0.08 to 0.4, and Reynolds numbers greater than about 20,000.

Simple geometries

For simple geometries, λ_{ij} was found to depend on the shape of the adjacent subchannel in addition to the c/d ratio. Hence, separate correlations were developed for each of the T-T, S-S, and S-T pairs.

Table 2: Summary of Correlations for λ_{ij}

Rogers' *simple* correlations:		Rehme's correlations:	
S-S:	$\lambda_{ij} = 0.0050(c/d)^{-0.894}$	S-S:	$\lambda_{ij} = 0.00531\{(1 + c/d)(c/d)\}^{-1}$
S-T:	$\lambda_{ij} = 0.0054(c/d)^{-0.950}$	S-T:	$\lambda_{ij} = 0.00673\{(1 + c/d)(c/d)\}^{-1}$
T-T:	$\lambda_{ij} = 0.0018(c/d)^{-1.40}$	T-T:	$\lambda_{ij} = 0.00921\{(1 + c/d)(c/d)\}^{-1}$
Rogers' *bundle* correlations:		Petrunik's correlations:	
S-S:	$\lambda_{ij} = 0.0058(c/d)^{-1.46}$	S-S	$\lambda_{ij} = 0.009(c/d)^{-1}$
S-T:	$\lambda_{ij} = 0.0058(c/d)^{-1.46}$	S-T	$\lambda_{ij} = 0.009(c/d)^{-1}$
T-T:	$\lambda_{ij} = 0.0058(c/d)^{-1.46}$	T-T	$\lambda_{ij} = 0.009(c/d)^{-1}$

The S-S expression was correlated by Rogers and Rosehart [7] using solely other researchers' data. The S-T and the T-T expressions were correlated by Rogers and Tahir [8]. For the T-T correlation Rogers and Tahir included their own data (one data point only) in addition to two researchers data. For the S-T correlation Rogers and Tahir used the data of Singh and St. Pierre [12], [13] as well as the data used originally by Rogers and Rosehart for a tentative S-T correlation. It should be noted that Rogers and Tahir also verified the Rogers and Rosehart S-S correlation with the inclusion of Singh and St. Pierre's data and found very good agreement.

3.2.2 Correlation of Petrunik. Petrunik [9] measured the mixing velocities for both single-phase and two-phase conditions in a T-T configuration. His single-phase measurements included water and Genetron-12 as working fluids. For his mixing correlation, however, he included other studies using both simple and bundle geometries. These studies encompassed the other configurations as well as additional gap-to-diameter ratios. He concluded that the mixing rate, $w_{ij}^{'}$, does *not* significantly depend on the gap-to-diameter ratio c/d.

From an experimental fit of the mixing velocity versus the Reynolds number, he determined:

$$\frac{w_{ij}^{'}}{\mu} = 0.009 Re^{0.827} \tag{17}$$

Thus, from Equation (7), the non-dimensional mixing length is:

$$\lambda_{ij} = 0.009(c/d)^{-1} \tag{18}$$

It should be observed that the Reynolds number exponent in the Petrunik correlation is not 0.9 as in the Rogers and co-workers models, but rather 0.827. This value was obtained directly from his subchannel measurements rather than from the pipe data of Knudsen. Most importantly, however, the mixing velocity is *not* a function of the c/d ratio or the subchannel type. The data base for this correlation includes S-S, S-T and T-T configurations.

3.2.3 Correlation of Rehme. Rehme [10] developed a model which provides a good approximation of the mixing rate for any gap geometry. The empirical component is entirely based on other researcher's data with a large overlap to those data used by Rogers and co-workers. It is also in essence the same model as developed by Ingesson and Hedberg [14].

As was shown earlier, the heat transported across the gap can be expressed as

$$Q_{ij} = (Lc)\rho c_p \bar{\epsilon}_{Hij} \left.\frac{dT}{dz}\right|_{ij}. \tag{19}$$

The gradient is approximated as

$$\left.\frac{dT}{dz}\right|_{ij} \approx \frac{T_i - T_j}{z_{ij}}, \tag{20}$$

Rehme sets the mixing distance, z_{ij}, equal to the distance between the centroids of the adjacent subchannels, δ_{ij}. The mean heat eddy-diffusivity is now expressed as $\bar{\epsilon}Y$, where $\bar{\epsilon}$ is a 'reference eddy viscosity' (for momentum) and Y is a 'mixing factor'. This mixing factor accounts for how much higher the actual mean heat eddy-diffusivity is in comparison with the reference eddy viscosity and also includes a correction for the linear temperature gradient approximation. The centroid distance is used for convenience. Thus,

$$Q_{ij} = (Lc)\rho c_p \bar{\epsilon} Y \frac{T_i - T_j}{\delta_{ij}}. \tag{21}$$

Rehme suggests that the reference eddy viscosity be given by the non-dimensional eddy viscosity at the center of a smooth circular tube, following Reichardt [15]. Rehme obtains:

$$\frac{\bar{\epsilon}}{\nu} = \frac{Re}{20}\sqrt{\frac{\lambda}{8}} \tag{22}$$

where:

$$\lambda = \text{Blasius friction factor} \tag{23}$$

$$= 4f = 4K_f Re^{-n} \tag{24}$$

and K_f =0.046 and n=0.2.

The factor of 20 appearing in Equation (22) is different from the factor obtained by the current authors when re-deriving that equation. Fundamentally, however, this does not alter the correlation since Y in Equation (21) is fitted experimentally.

Empirical fit for Y

Using available data from the literature (including the data used by Rogers and co-workers), and data for all gap geometries, Rehme arrives at the following correlation for the mixing factor:

$$Y = \frac{0.7}{\frac{c}{d}}. \tag{25}$$

By substituting Equations (22) to (25) into Equation (21), and noting that $\Delta h = C_p \Delta T$, the turbulent heat transfer across the gap can be written as:

$$Q_{ij} = L\frac{c}{\delta_{ij}}\frac{0.00531}{c/d}\mu Re^m (h_i - h_j) \tag{26}$$

where $m = 1 - n/2 = 0.9$ (usually). Hence:

$$\frac{w'_{ij}}{\mu} = (\frac{d}{\delta_{ij}})0.00531 Re^m \tag{27}$$

The ratio of the fuel rod diameter, d, to the centroidal distance, δ_{ij}, must be defined. By considering rod configurations with uniform rod diameters and gaps, the following ratios can be defined:

$$\text{S-S:} \quad \frac{d}{\delta_{ij}} = \left(1+\frac{c}{d}\right)^{-1} \tag{28}$$

$$\text{T-T:} \quad \frac{d}{\delta_{ij}} = 1.732\left(1+\frac{c}{d}\right)^{-1} \tag{29}$$

$$\text{S-T:} \quad \frac{d}{\delta_{ij}} = 1.267\left(1+\frac{c}{d}\right)^{-1} \tag{30}$$

Thus, the mixing rate $w_{ij}^{'}$ for each subchannel configuration is given as:

$$\text{S-S:} \quad \frac{w_{ij}'}{\mu} = 0.00531\left(\frac{1}{1+c/d}\right)Re^m \tag{31}$$

$$\text{T-T:} \quad \frac{w_{ij}'}{\mu} = 0.00921\left(\frac{1}{1+c/d}\right)Re^m \tag{32}$$

$$\text{S-T:} \quad \frac{w_{ij}'}{\mu} = 0.00673\left(\frac{1}{1+c/d}\right)Re^m \tag{33}$$

The corresponding equations for λ_{ij} are given by:

$$\text{S-S:} \quad \lambda_{ij} = 0.00531\left\{(1+c/d)(c/d)\right\}^{-1} \tag{34}$$

$$\text{T-T:} \quad \lambda_{ij} = 0.00921\left\{(1+c/d)(c/d)\right\}^{-1} \tag{35}$$

$$\text{S-T:} \quad \lambda_{ij} = 0.00673\left\{(1+c/d)(c/d)\right\}^{-1} \tag{36}$$

$$\tag{37}$$

It should be noted that Rehme does not specify how the Reynolds number is calculated. For 'simple' twin S-S and T-T configurations the Reynolds number in adjacent subchannels should be the same. For S-T configurations, correction is required. This correction is discussed in detail in the following section.

4. CORRECTIONS FOR UNEQUAL REYNOLDS NUMBERS IN S-T SUBCHANNEL PAIRS

The general formulation for the turbulent mixing rate is given by:

$$\frac{w_{ij}^{'}}{\mu} = \frac{c}{d}\lambda_{ij}Re^m \tag{38}$$

where $m = 1 - n/2$. The Reynolds number in Equation (38) is representative of the Reynolds numbers in the two adjacent subchannels i and j. This Reynolds number can be evaluated using different methods:

$$\text{Method 1:} \quad Re = \left(\frac{Re_i^m + Re_j^m}{2}\right)^{1/m} \tag{39}$$

$$\text{Method 2:} \quad Re = \frac{\rho U_{i+j} D_{i+j}}{\mu} \tag{40}$$

With Method 2 the two subchannels are effectively combined to make one large subchannel, thus U_{i+j} and D_{i+j} are the average velocity and the hydraulic diameter, respectively, for the combined subchannel.

It is desired to determine a correction factor, K, such that:

$$Re = KRe_i \tag{41}$$

where Re_i is the Reynolds number in the square subchannel (subchannel i).

To derive a correction factor for each method of calculating Re, the following relationships are required:

For a Square Subchannel (i):

$$P_i = \text{wetted perimeter} = \pi d \tag{42}$$

$$A_i = \text{flow area} = (c+d)^2 - \frac{\pi}{4}d^2 \tag{43}$$

$$D_i = \text{hydraulic diameter} = d\left\{\left(\frac{4}{\pi}\right)\left(1+\frac{c}{d}\right)^2 - 1\right\} \tag{44}$$

For a Triangular Subchannel (j):

$$P_j = \text{wetted perimeter} = \frac{\pi d}{2} \tag{45}$$

$$A_j = \text{flow area} = \frac{\sqrt{3}}{4}(c+d)^2 - \frac{\pi}{8}d^2 \tag{46}$$

$$D_j = \text{hydraulic diameter} = d\left\{\left(\frac{2\sqrt{3}}{\pi}\right)\left(1+\frac{c}{d}\right)^2 - 1\right\} \tag{47}$$

Also required is the ratio of the Reynolds numbers in subchannels i and j. This ratio can be found by considering fully developed flow in parallel subchannels subjected to the same pressure drop. From such an analysis the following relationship can be deduced:

$$\frac{Re_j}{Re_i} = \left(\frac{D_j}{D_i}\right)^{\frac{3}{2-n}} \tag{48}$$

where n is the exponent in the friction factor correlation and is usually taken to be 0.2.

4.1 Reynolds Number Correction for Method 1

By using Method 1 to calculate the Reynolds number, it is seen that:

$$Re^m = \frac{Re_i^m + Re_j^m}{2} \tag{49}$$

$$= \left(\frac{1+\left(\frac{Re_j}{Re_i}\right)^m}{2}\right) Re_i^m \tag{50}$$

But applying Equation (48) yields:

$$Re^m = \left(\frac{1+\left(\frac{D_j}{D_i}\right)^{\left(\frac{3m}{2-n}\right)}}{2}\right) Re_i^m \tag{51}$$

The mixing velocity, $w_{ij}^{'}$, for S-T subchannels can therefore be written as:

$$w_{ij}^{'} = \left(\frac{c}{d}\right)\lambda_{ij} K_c^{'} Re_i^m \tag{52}$$

where:

$$K_c^{'} = \frac{1}{2}\left\{1 + \left(\frac{D_j}{D_i}\right)^{\frac{3m}{2-n}}\right\} \tag{53}$$

and

$$\frac{D_j}{D_i} = \left(\frac{1.1027(1+\frac{c}{d})^2 - 1}{1.2732(1+\frac{c}{d})^2 - 1}\right) \tag{54}$$

4.2 Reynolds Number Correction for Method 2

The second method for calculating the Reynolds number is to combine the two adjacent subchannels into a single larger subchannel. Hence,

$$Re^m = (Re_{i+j})^m = \left(\frac{Re_{i+j}}{Re_i}\right)^m Re_i^m \tag{55}$$

where:

$$Re_{i+j} = \frac{\rho}{\mu} V_{i+j} D_{i+j} = \frac{\rho}{\mu}\left(\frac{\dot{m}_i + \dot{m}_j}{\rho(A_i + A_j)}\right) D_{i+j} \tag{56}$$

Note that Equation (56) presumes that the density and viscosity in each subchannel are the same.

By noting that:

$$D_{i+j} = \frac{4(A_i + A_j)}{(P_i + P_j)} \tag{57}$$

$$\dot{m}_i = Re_i\left(\frac{\mu A_i}{D_i}\right) \tag{58}$$

$$\dot{m}_j = Re_j\left(\frac{\mu A_j}{D_j}\right) \tag{59}$$

$$\frac{P_j}{P_i} = 0.5 \tag{60}$$

The combined Reynolds number can be written as:

$$Re_{i+j} = \left(\frac{2}{3}\right)\left(1 + \frac{1}{2}\left(\frac{D_j}{D_i}\right)^{\frac{3}{2-n}}\right) Re_i \tag{61}$$

Hence, the mixing velocity can be written as:

$$w_{ij}^{'} = \frac{c}{d}\lambda_{ij} K_c^{"} Re_i^m \tag{62}$$

where:

$$K_c^{"} = \left\{\left(\frac{2}{3}\right)\left(1 + \frac{1}{2}\left(\frac{D_j}{D_i}\right)^{\frac{3}{2-n}}\right)\right\}^m \tag{63}$$

and

$$\frac{D_j}{D_i} = \left(\frac{1.1027(1+\frac{c}{d})^2 - 1}{1.2732(1+\frac{c}{d})^2 - 1}\right) \tag{64}$$

4.3 Application of Reynolds Number Correction to Correlations

In the Rogers and co-workers model the Reynolds number is calculated using Method 1. Following the methodology used in ASSERT-PV, the Petrunik model is calculated here using Method 2. Rehme is ambiguous as to the calculation of the Reynolds number. In the current paper, we will use Method 1 for Rehme's correlation.

As discussed earlier, for the twin S-S and T-T configurations, the two methods are identical since $D_i = D_j$. A summary of the final expressions for w'_{ij} is given in Table 3.

5. COMPARISON OF MIXING MODELS

Figures 2 and 3 show the turbulent mixing rate, w'_{ij}, as a function of Reynolds number for c/d values of 0.1 and 0.2, respectively. All three geometrical configurations are shown. Several observations can be made:

1. The influence of the c/d ratio is much larger for the Rogers' bundle model than for any of the others.
2. For both the S-S and the S-T configurations, the Rogers' simple, Rehme's and Petrunik's models are very close and distinctly separate from Rogers' bundle model. In the T-T configuration, Rehme lies somewhere in the middle.
3. Rogers' bundle model consistently predicts the highest mixing velocities.
4. Petrunik's model is of course nominally independent of the c/d ratio. For the S-T configuration, however, a slight c/d dependence due to the asymmetry is apparent.
5. Except for Rogers' bundle and Rogers' simple T-T all correlations are very insensitive to the c/d ratio - much less than to the Reynolds number. This is an observation often mentioned in the literature.

6. VALIDITY OF CORRELATIONS FOR STEAM FLOWS

In this section the validity of the turbulent thermal mixing correlations for single-phase steam conditions is discussed. The discussion is based on the underlying similarity to a pipe flow and by experimental verification with other gas flows. These two approaches are presented separately below.

6.1 Comparison to Pipe Flow

The fundamental assumption of the subchannel thermalhydraulic modelling is that the subchannel flow is equivalent to a pipe flow based on the equivalent subchannel hydraulic diameter. With this assumption, both pressure losses and turbulent mixing are being evaluated. This assumption of equivalency is supported by experimental evidence which suggests that measured friction factors in subchannels (i.e., pressure losses) agree well with those from a round pipe evaluated with an equivalent subchannel hydraulic diameter. Rogers and Tahir [8], for example found that $f = 0.44Re^{-0.194}$ which is very close to the correlation for smooth tubes as given by Knudsen [11]. Their c/d ratio was 0.4. Rehme [16] examined this issue in detail and found that:

> 'For the pressure-drop coefficient [friction factor] there is a rapid increase from 60% of the circular tube value at a rod distance of $c/d = 0$ to approximately 100% at

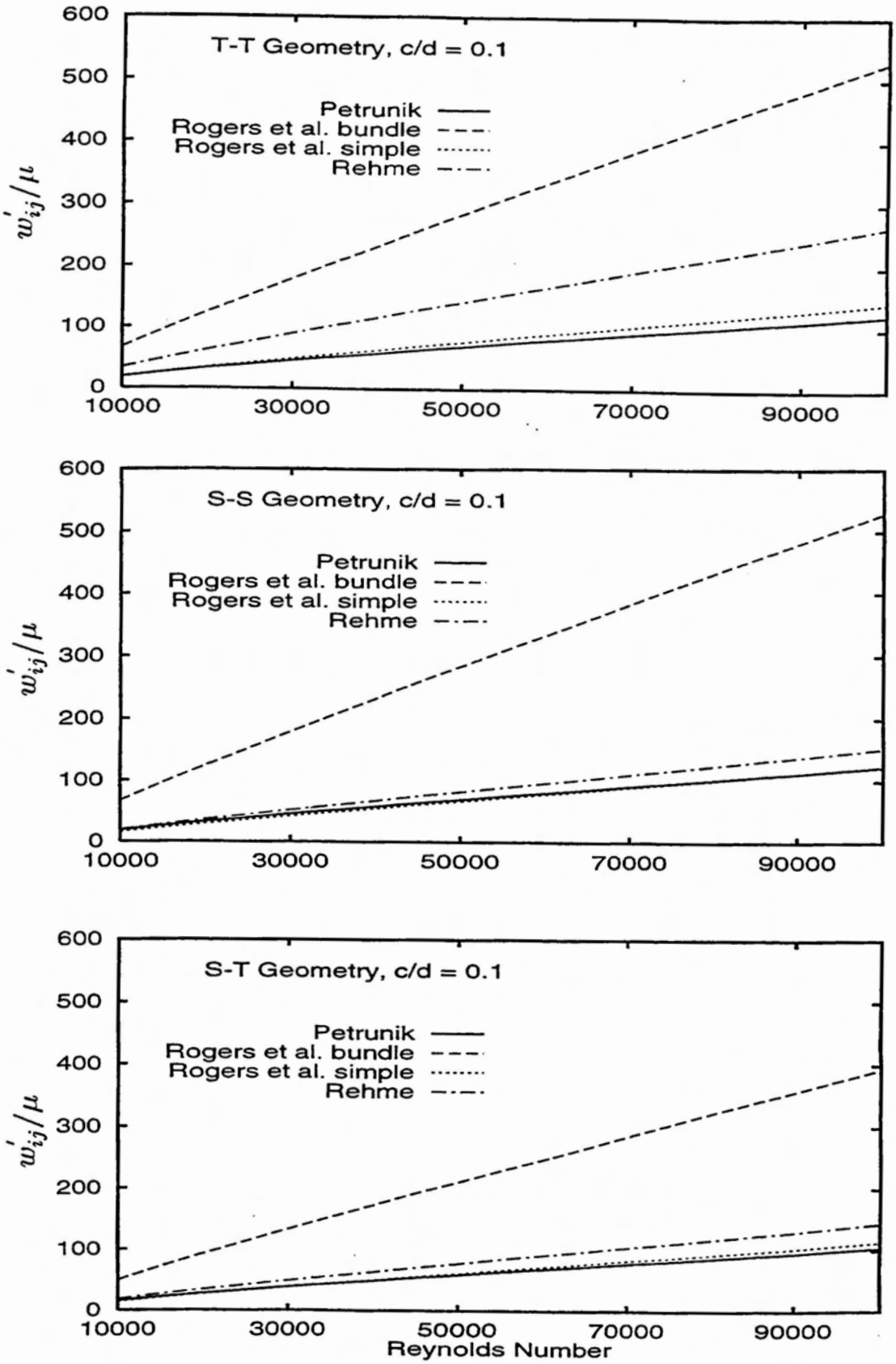

Figure 2: Mixing velocity versus Reynolds number for c/d=0.1.

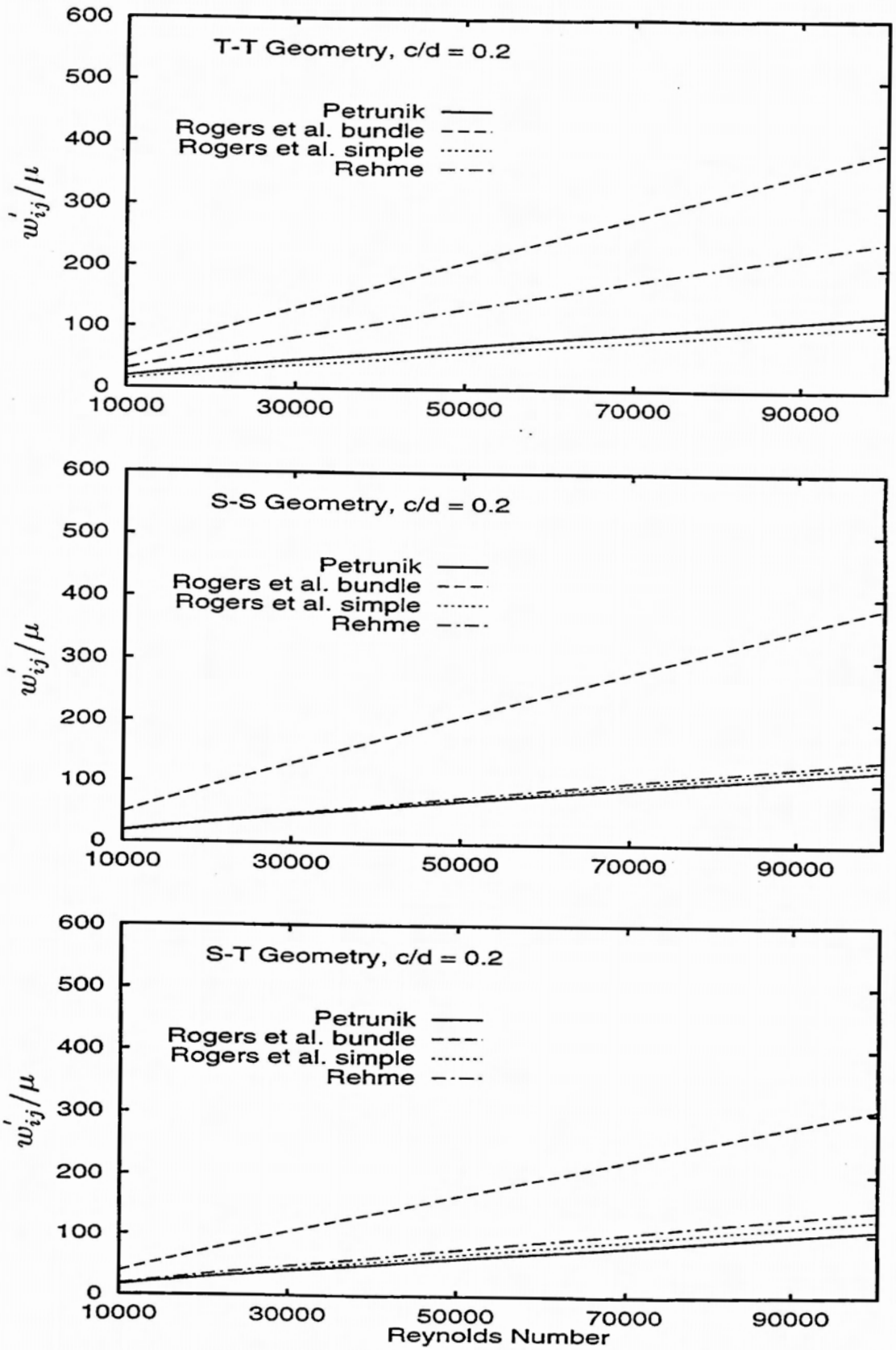

Figure 3: Mixing velocity versus Reynolds number for c/d=0.2.

Table 3: Summary of Correlations for w'_{ij}

	Rogers' *simple* correlations:		Rehme's correlations:
S-S	$\frac{w'_{ij}}{\mu} = 0.0050 Re_i^{0.9} \left(\frac{c}{d}\right)^{0.106}$	S-S	$\frac{w'_{ij}}{\mu} = 0.00531 \left(\frac{1}{1+c/d}\right) Re_i^{0.9}$
S-T	$\frac{w'_{ij}}{\mu} = 0.0054 Re_i^{0.9} \left(\frac{c}{d}\right)^{0.050} K'_c$	S-T	$\frac{w'_{ij}}{\mu} = 0.00673 \left(\frac{1}{1+c/d}\right) Re_i^{0.9} K'_c$
T-T	$\frac{w'_{ij}}{\mu} = 0.0018 Re_i^{0.9} \left(\frac{c}{d}\right)^{-0.4}$	T-T	$\frac{w'_{ij}}{\mu} = 0.00921 \left(\frac{1}{1+c/d}\right) Re_i^{0.9}$
	Rogers' *bundle* correlations:		Petrunik's correlations:
S-S	$\frac{w'_{ij}}{\mu} = 0.0058 Re_i^{0.9} \left(\frac{c}{d}\right)^{-0.46}$	S-S	$\frac{w'_{ij}}{\mu} = 0.009 Re_i^{0.827}$
S-T	$\frac{w'_{ij}}{\mu} = 0.0058 Re_i^{0.9} \left(\frac{c}{d}\right)^{-0.46} K'_c$	S-T	$\frac{w'_{ij}}{\mu} = 0.009 Re_i^{0.827} K_c$"
T-T	$\frac{w'_{ij}}{\mu} = 0.0058 Re_i^{0.9} \left(\frac{c}{d}\right)^{-0.46}$	T-T	$\frac{w'_{ij}}{\mu} = 0.009 Re_i^{0.827}$

where:

$$K'_c = \frac{1}{2}\left\{1 + \left(\frac{1.1027\,(1+c/d)^2 - 1}{1.2732\,(1+c/d)^2 - 1}\right)^{1.5}\right\} \quad \text{and} \quad K''_c = \left\{\left(\frac{2}{3}\right)\left(1 + \frac{1}{2}\left(\frac{D_j}{D_i}\right)^{\frac{5}{3}}\right)\right\}^{0.827}$$

with

$$\frac{D_j}{D_i} = \frac{1.1027\,(1+c/d)^2 - 1}{1.2732\,(1+c/d)^2 - 1}$$

$c/d \approx 0.08$. For higher rod distance ratios, the pressure-drop coefficient increases to only some 110% of the tube value for $c/d = 1$.' [16]

This agrees with Rogers and Tahir's results at their relatively high c/d ratio.

The frictional losses are a function of the eddy viscosity in the radial direction, defined by

$$\epsilon_{mr} = -\frac{\overline{u'v'}}{\frac{\partial \overline{u}}{\partial y}},$$

where y and v are normal to the rod. One would expect that these eddy viscosities are close to those in a pipe, given the foregoing results of Rogers and Tahir, and Rehme. Meyer [17] examined a central channel of a 37-rod bundle with $c/d = 0.12$ and did indeed find that the radial eddy viscosity is close to Reichardt's circular pipe data (although slightly higher) and not a function of azimuthal direction.

While the radial eddy viscosity is similar to that in a pipe, the azimuthal eddy-viscosity tends to be larger in a subchannel than in a circular pipe, especially near the gap region. In other words, the anisotropy or the ratio of the azimuthal to the radial eddy-viscosity is larger in subchannels. The azimuthal eddy-viscosity is defined by

$$\epsilon_{ma} = -\frac{\overline{uw}}{\frac{1}{r}\frac{\partial \overline{u}}{\partial \phi}},$$

where w is the velocity component parallel to the rod wall, r is the distance from the center of the rod and ϕ is the azimuthal angle.

Meyer [17], for example, found that the azimuthal eddy-viscosity is higher than the radial eddy-viscosity away from the rod, especially in the gap region, perhaps by a factor of 3 or 4, whereas in a pipe this ratio is at most about 2 [19]. In a wall channel of the 37-rod bundle, with a wall-to-diameter ratio of 0.06, the ratio was even higher, up to about 200 in the gap between the wall and the rod (Krauss and Meyer [18]).

At the core of all three models is essentially the same form of the eddy-viscosity model:

$$\frac{\varepsilon_t}{\nu} = K' Re^m, \tag{65}$$

In the models, the anisotropy or specifically the differences between the given eddy-viscosities and those occurring in the subchannels, are accounted for in a lumped-parameter analysis by empirically fitting the data with the help of 'adjustment factors' which depend on the subchannel geometry. The lumping and fitting also accounts for the spatial variations of the eddy-viscosity. In the Rogers model, the adjustment factor is introduced via the non-dimensional mixing distance (λ_{ij}), and in the Rehme model, where the mixing distance is assumed to be the centroid-to-centroid distance (δ_{ij}), the adjustment factor is introduced via the mixing factor (Y). These adjustment factors take into account the geometric dependence of the eddy-viscosity by fitting a functional dependence on the c/d ratio. The proportionality constants in these adjustment factors account for the spatial averaging of the eddy-viscosity.

The Reynolds-number dependence of the above models, on the other hand, is independently introduced via the friction-factor relationship, i.e., the Reynolds number exponent $m = 1 - n/2$ in the above equations is obtained from $f = K_f Re^{-n}$.[2] This relationship is independent of the anisotropy, the geometric dependence (c/d), or the spatial variation.

To answer the question of whether or not steam can be used in the models, is tantamount to asking whether the above Reynolds-number dependence is correct, or, more specifically, whether the eddy-viscosity depends on any other fluid-property dependent parameters. The above discussion demonstrates that there is no reason to believe that the eddy-viscosity depends on any other fluid-property dependent parameter except the Reynolds number, much like circular-pipe flow, open-channel flow, rectangular-channel flow or boundary-layer flow. To be sure, anisotropies, geometric dependence and spatial dependence will differ, but these can be independently accounted for, by, in a sense, adjusting the K 'constants' above. Given that the eddy-viscosities depend on the Reynolds number and no other fluid-property dependent parameter, dynamic similarity through the use of the Reynolds numbers assures us that any fluid can be used. It should be noted that to the extent that the Reynolds-number exponent m is inaccurate, the final mixing velocity is no less accurate for one fluid versus another.

6.2 Correlations with Air Data

As final verification that the models are valid for steam, the correlations will be compared to the available data on air. This is a reasonable comparison, given that both fluids can be treated as ideal gases with similar Prandtl numbers.

Figure 4 shows the correlations and experimental data for the symmetric S-S configuration, Figure 5 for the asymmetric S-T configuration, and Figure 6 for the symmetric T-T configuration. The experimental data, denoted by the symbols, are summarised in Table 4. The quantity λ_{ij} is considered since it is independent of the Reynolds number. As discussed earlier, the Reynolds

[2]Petrunik determines the exponent m directly from the mixing data and in fact obtains a constant (0.827) which is close to the one obtained from the friction factor's Reynolds number exponent m. A fit of Rogers and Tahir's data (w'_{ij} versus Re_i) revealed that $m = 1.0$ - but they did not do this for their correlation, although it would have improved the independence of the Reynolds number for λ_{ij}.

Table 4: Experimental-data summary

Symbol	Reference	Fluid	Source	Their Ref.
B	Bowring (1969)	Freon	Rogers and Rosehart [7]	(19)
BA	Bishop et al. (1962)	H_2O	Rogers and Rosehart [7]	(15)
BR	Biggs and Rust (1967)	H_2O	Rogers and Rosehart [7]	(17)
C	Clarke (1961)	H_2O	Rogers and Rosehart [7]	(10)
CF	Collins and France (1958)	Air	Rogers and Rosehart [7]	(14)
H	Hetsroni et al. (1968)	H_2O	Rogers and Rosehart [7]	(18)
K	Kielstrom (1972)	Air	Rogers and Tahir [8]	(8)
N	Nelson et al. (1960)	H_2O	Rogers and Rosehart [7]	(16)
P	Petrunik (1973)	H_2O	Rogers and Tahir [8]	(9)
R	Roidt et al. (1973)	Air	Rogers and Rosehart [7]	(11)
RA	Rowe and Angle (1967)	H_2O	Rogers and Rosehart [7]	(7)
RT	Rogers and Tahir [8]	Air	Rogers and Tahir [8]	
RP	Rapier (1967)	Air	Rogers and Rosehart [7]	(12)
S	Seale [19]	Air	Seale [19]	
T	Rogers and Tarasuk (1966)	H_2O	Rogers and Rosehart [7]	(2)

number dependence usually comes directly from the friction factor relationship and is *not* fitted empirically (except by Petrunik). The actual empirical fits are made directly (Rogers and co-workers), or indirectly (Rehme, Petrunik), with regard to λ_{ij}. Thus, it makes most sense to compare the models in conjunction with data on this basis.

Unfortunately, no air data was available for the S-T configuration. Nevertheless, there is no reason to believe the general agreement would different for this configuration.

Again, with a global perspective, it is noted that all data fall within the range of the correlations, as expected. More specifically, *both* the air and the water data fall within the range. Thus, there is no evidence to suggest that air data somehow behaves differently. Furthermore, the majority of the air data, except that by Collins and France, fall closer to Rogers's simple correlation. This includes the most recent data available, by Seale [19]. Rehme's correlation appears to overestimate the available data for higher c/d ratios in the T-T configuration, but agrees well in the S-S configuration. It should also be observed that the data by Rapier, which Rogers classified as bundle data, actually falls closer to the simple correlation (in the S-S configuration).

In summary, it can be concluded that the experimental data supports the earlier conclusion that the mixing for a gas, in this case air, would be well predicted within the accuracy of the correlations, just as well as for liquid water.

7. SUMMARY

This paper has been concerned with mathematical modelling of the turbulent transport of energy in subchannel geometries. The specific intents were to compare existing correlations for turbulent thermal mixing and to determine the applicability of the correlations to flows of superheated steam.

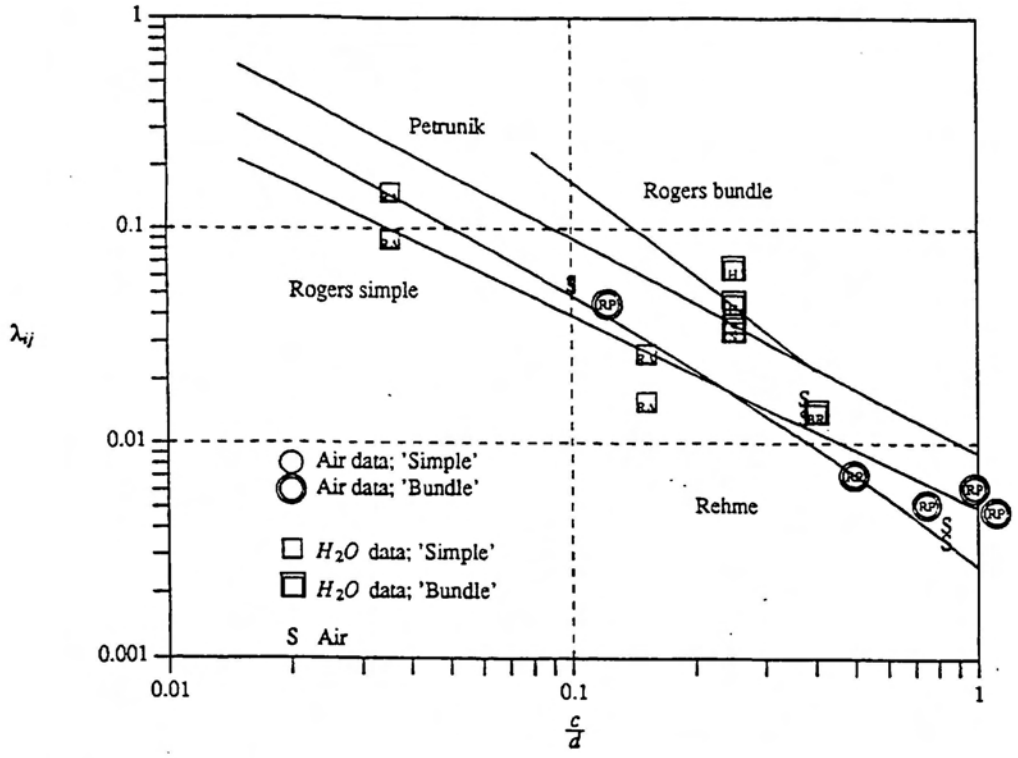

Figure 4: Non-dimensional mixing distance versus gap-to-rod diameter ratio for S-S geometries.

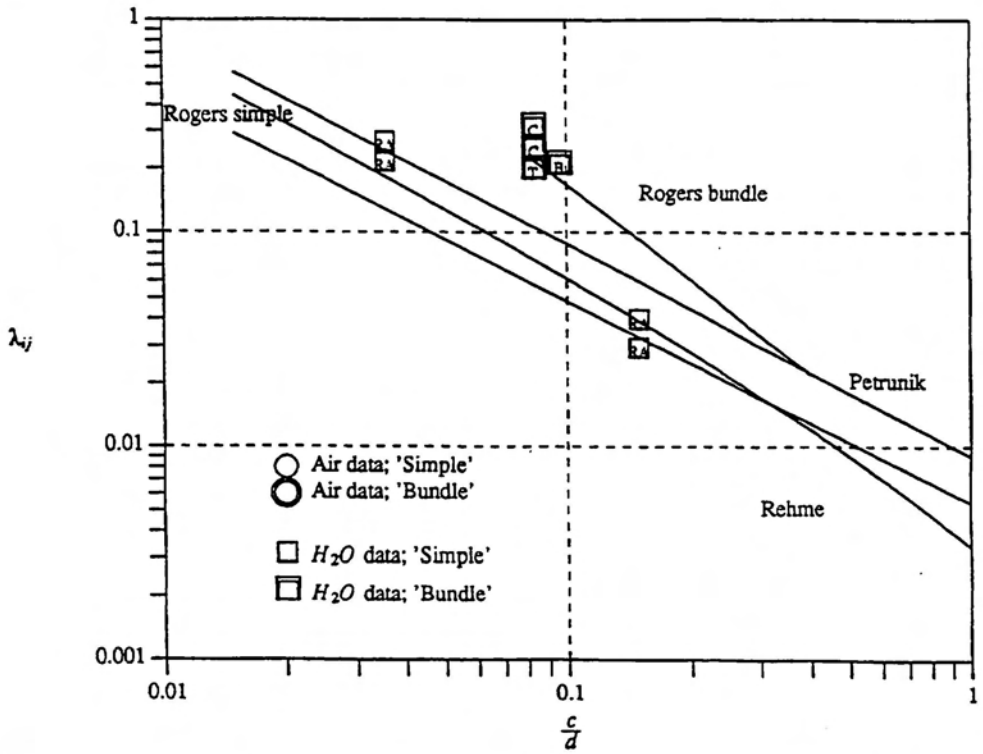

Figure 5: Non-dimensional mixing distance versus gap-to-rod diameter ratio for S-T geometries.

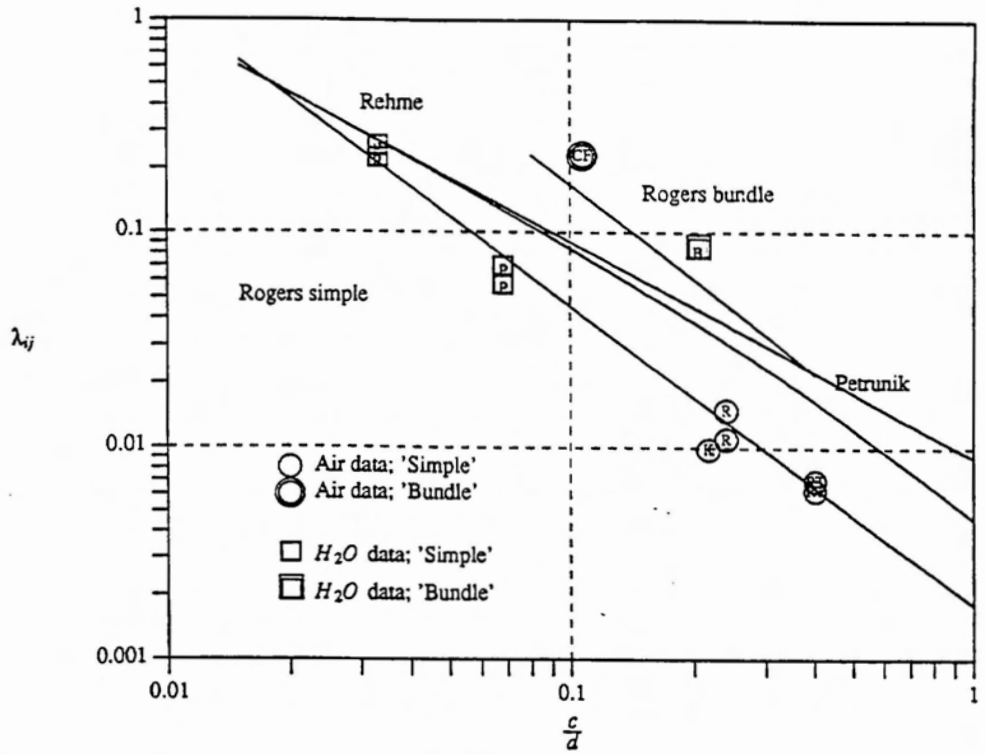

Figure 6: Non-dimensional mixing distance versus gap-to-rod diameter ratio for T-T geometries.

The correlations for the mixing rate, w'_{ij}, are typically a function of the Reynolds number of the flow and the ratio of the gap spacing, c, to the fuel rod diameter d. Of the correlations considered in this work (Rogers and co-workers [7] [8], Petrunik [9], and Rehme [10], the same (or very similar) Reynolds number dependence was used. Further, Rogers and co-workers distinguished between simple and bundle geometries, whereas the others did not. The Rogers bundle correlation consistently predicts the highest mixing rate and also shows the greatest sensitivity to the value of c/d. Petrunik's model and Roger's model for simple geometries provided the lowest values of the mixing rate.

The applicability of the models to steam flows was assessed by considering both the derivations of the correlations and experimental data for flows of air. From consideration of the derivation, there is no basis for restricting the models to liquid flows only. Further, comparison of the correlation predictions to experimental data for air flows (for S-S and T-T geometries) shows that the data fall within the range of the correlations. Thus, it is concluded that the correlations are equally valid for vapour as for liquid water.

References

[1] CARVER M.B., KITELEY J.C., TAHIR A., BANAS A.O., and ROWE D.S., 'Simulation of Flow and Phase Distribution in Vertical and Horizontal Bundles using the ASSERT Subchannel Code', Nuclear Engineering and Design, Vol. 122, pp. 413-424 1990.

[2] LIGHTSTONE M.F., and ROCK R.C.K., 'Investigation of Coolant Thermal Mixing within 28-Element CANDU Fuel Bundles using the ASSERT-PV Thermalhydraulic Code', presented at the 17th Annual CNS Conference, Fredericton, New Brunswick, June 9-12 1996.

[3] WESTBYE C.J., BRITO A.C., MACKINNON J.C., SILLS H.E., and LANGMAN V.J., 'Development, Verification and Validation of the Fuel Channel Behaviour Computer Code FACTAR', presented at the 35th Annual CNA/CNS Conference, Saskatoon, Saskatchewan, June 4-7 1995.

[4] HARVEL G.D., DAM R., SOULARD M., and GIBB R.A., 'Investigation of Flow Blockage in a Fuel Channel with the ASSERT Subchannel Code', presented at the 17th Annual CNS Conference, Fredericton, New Brunswick, June 9-12 1996.

[5] DIMMICK G.R., CARVER M.B., LIGHTSTONE M.F., LUX E.G., and JUNOP, S., 'Bundle Thermalhydraulic Experiments and Code Validation in Support of Design and Licensing of the MAPLE-X10 Reactor', presented at 'New Trends in Nuclear System Thermalhydraulics', Pisa, Italy, May 30-June 2, 1994.

[6] CARVER M.B., KITELEY J.C., ZHOU Q-N, and JUNOP S.V., *Nuclear Technology*, Vol. 112, pp 299-314, 1995.

[7] ROGERS, J.T. and ROSEHART, R.G., 'Mixing by Turbulent Interchange in Fuel Bundles. Correlations and Inferences', *ASME* paper 72-HT-53, 1972.

[8] ROGERS, J.T. and TAHIR, A.E.E., 'Turbulent Interchange Mixing in Rod Bundles and the Role of Secondary Flows', *ASME* paper 75-HT-31, 1975.

[9] PETRUNIK, K., 'Turbulent Interchange in Simulated Rod Bundle Geometries for Genetron-12 Flows', Ph.D. thesis, U. of Windsor, Ontario, Canada, 1973.

[10] REHME, K., 'The Structure of Turbulence in Rod Bundles and the Implications on Natural Mixing Between the Subchannels', Int. J. Heat Mass Transfer, Vol. 37, No.2, pp. 567-581, 1992.

[11] KNUDSEN, J.G., and KATZ, D.L. 'Fluid Dynamics and Heat Transfer', McGraw-Hill Book Company, Toronto. pg. 173., 1958.

[12] SINGH, K. 'Air-Water Turbulent Interchange Mixing in Simulated Rod-Bundle Geometries', Ph.D. Thesis, Dept. of Chemical Engineering, University of Windsor, Ont. June, 1972.

[13] SINGH, K. and ST. PIERRE, C.C., 'Single Phase Turbulent Mixing in Simulated Rod Bundle Geometries', Transactions of the Canadian Society of Mechanical Engineering, Vol 1 No. 2, pp. 73-80 June, 1972.

[14] INGESSON, L. and HEDBERG, S., 'Heat Transfer Between Subchannels in a Rod Bundle', Heat Transfer 1970, Paris, Vol. III, FC7.11 Elsevier, Amsterdam 1970.

[15] REICHARDT, H., Vollständige Darstellung der turbulenten Geschwindigkeiten in glatten Leitungen, Z. angew. Math. Mech., Bd. 31, Nr. 7, 208-219, 1951.

[16] REHME, K., 'Pressure Drop Performance of Rod Bundles in Hexagonal Arrangements', Int. J. Heat Mass Transfer, Vol. 15, pp. 2499-2517. 1972.

[17] MEYER, L. 'Measurements of Turbulent Velocity and Temperature in Axial Flow Through a Heated Rod Bundle', Nuclear Engineering and Design, Vol. 146, pp. 71-82. 1994.

[18] KRAUSS, T. and MEYER, L., 'Characteristics of Turbulent Velocity and Temperature in a Wall Channel of a Heated Rod Bundle', Experimental Thermal and Fluid Science, Vol. 12, 75-86, 1996.

[19] SEALE, W.J., 'Turbulent Diffusion of Heat Between Connected Flow Passages - Part I: Outline of Problem and Experimental Investigation', Nuclear Engineering and Design, Vol. 54, pp. 183-195. 1979.